Anisotropic Mechanical Properties of Tissue Components in Human Atherosclerotic Plaques

Gerhard A. Holzapfel[1]
Mem. ASME

Gerhard Sommer
Mem. ASME

Graz University of Technology,
Institute for Structural Analysis,
Computational Biomechanics,
Schiesstattgasse 14-B, 8010 Graz, Austria

Peter Regitnig
Mem. ASME
Medical University Graz, Institute of Pathology,
Auenbruggerplatz 25, 8036 Graz, Austria

Knowledge of the biomechanical properties of human atherosclerotic plaques is of essential importance for developing more insights in the pathophysiology of the cardiovascular system and for better predicting the outcome of interventional treatments such as balloon angioplasty. Available data are mainly based on uniaxial tests, and most of the studies investigate the mechanical response of fibrous plaque caps only. However, stress distributions during, for example, balloon angioplasty are strongly influenced by all components of atherosclerotic lesions. A total number of 107 samples from nine human high-grade stenotic iliac arteries were tested; associated anamnesis of donors reported. Magnetic resonance imaging was employed to test the usability of the harvested arteries. Histological analyses has served to characterize the different tissue types. Prepared strips of 7 different tissue types underwent cyclic quasistatic uniaxial tension tests in axial and circumferential directions; ultimate tensile stresses and stretches were documented. Experimental data of individual samples indicated anisotropic and highly nonlinear tissue properties as well as considerable interspecimen differences. The calcification showed, however, a linear property, with about the same stiffness as observed for the adventitia in high stress regions. The stress and stretch values at calcification fracture are smaller (179 ± 56 kPa and 1.02 ± 0.005) than for each of the other tissue components. Of all intimal tissues investigated, the lowest fracture stress occurred in the circumferential direction of the fibrous cap (254.8 ± 79.8 kPa at stretch 1.182 ± 0.1). The adventitia demonstrated the highest and the nondiseased media the lowest mechanical strength on average. [DOI: 10.1115/1.1800557]

1 Introduction

Atherosclerosis is a vascular disease associated with the accumulation of lipids leading to invasion of leucocytes and smooth muscle cells into the intima, a process which may proceed in the formation of atheroma. Biomechanical and biochemical mechanisms are then involved in the development of a lesion known as an atherosclerotic plaque, which is composed primarily of fibrous tissue of varying density and cellularity. In addition, calcium, extracellular lipid, and lipid-laden foam cells are present, each constituting 5%–10% of the remaining area. Advanced atherosclerosis may lead to lesions which can reduce or block the flow of the oxygen-containing blood leading to oxygen deficiency in the tissues. Clinical emergencies such as myocardial infarction and stroke can result from plaque rupture and subsequent release of highly thrombogenic material and lipids into the blood stream. It is important to point out that the danger of suffering a myocardial infarction or a stroke is particularly high in cases of unstable or vulnerable plaques, which are thought to have a thin fibrous cap, a large lipid core, and significant inflammatory cell infiltration (see, for example, Refs. [1–3]). Atherosclerotic cardiovascular disease remains the leading cause of death and disability in North America [4]. In all European countries cardiovascular disease is the main cause of death in women and the main cause of death in men except in France [5].

A frequently used and well-established therapeutical intervention for reducing the severity of atherosclerotic plaques is balloon angioplasty with or without stenting (see Ref. [6], and references therein). It represents a mechanical solution for a clinical problem in which, for example, disease-free (medial) tissue is overstretched (damaged), plaques are disrupted or dissected, and redistribution inside the wall and lipid extrusion occur. These mechanisms alter the mechanical environment such that a cascade of biological responses occur, which may cause restenosis or thrombosis. Besides the knowledge of the composition and the geometry of the plaque, applied loads and parameters of balloon catheters and stents, it is the detailed information on the biomechanical behaviors of atherosclerotic plaques and nondiseased cardiovascular tissues that is crucial for a complete mechanical description of this interventional procedure. Understanding of the mechanical behavior of plaques under various loading conditions is an essential contributor for developing more insight in the physiology and pathophysiology of the cardiovascular system and new procedures for preventing or reducing restenosis, and for better predicting the outcome of interventional treatments on a plaque- or patient-specific basis.

To motivate further the need to understand the constitutive behavior of atherosclerotic plaque, consider the following recent statement by Richardson [7]: ''*There are relatively few data on the mechanical properties of arterial tissues, especially for the separate layers of a vessel wall, and the materials-testing protocols have varied between the measurements that have been published. This is probably the most uncertain aspect in the whole body of study of plaque fracture.*''

We summarize now the work performed on mechanical plaque testing and data available in the literature (see also the surveys [8,9]). The first uniaxial tensile tests on ulcerated and nonulcerated thoracic plaque caps and adjacent intima from human aortae seem to have been performed by Lendon et al. [10]. Results showed marked differences between plaques and heterogeneity within individual plaque caps. Fracture stresses ranged from 12 to 1938 kPa. Uniaxial tension tests on axial strips of aortic plaques were also performed by Born and Richardson [11], although little detail was provided of the results. Lendon et al. [12] compared

[1]Author to whom correspondence should be addressed. Phone: ++43 316 873 1625; Fax: ++43 316 873 1615; e-mail: gh@biomech.tu-graz.ac.at

Contributed by the Bioengineering Division for publication in the JOURNAL OF BIOMECHANICAL ENGINEERING. Manuscript received by the Bioengineering Division February 16, 2004; revised received April 16, 2004. Associate Editor: J. D. Humphrey.

Table 1 Anamnesis: CIA, common iliac artery; EIA, external iliac artery; IIA, internal iliac artery; AH, antihypertensives; AS, atherosclerosis; BP, bronchopneumonia; BS, bypass surgery; CS, coronary sclerosis; GHD, global heart dilation; GS, generally atherosclerosis; MI, myocardial infarction. Types of atherosclerotic lesions are according to Stary et al. [22]. Assessment of atherosclerosis is based on autopsy reports (y, medium or high grade; n, no or low grade).

Specimen	I	II	III	IV	V	VI	VII	VIII	IX
Type of iliac artery	EIA	CIA	IIA	CIA	CIA	IIA	CIA	IIA	CIA
Age (yrs)	65	90	80	64	81	60	60	87	87
Sex	f	m	f	f	f	m	m	f	f
Primary disease	CS	GS	AS	CS	CS	CS	AS	GS	GS
Cause of death	MI	MI	BP	MI	MI	GHD	MI	BP	BP
Atherosclerosis									
Type of atherosclerotic lesions [22]	*V*	*VII*	*V*	*VIII*	*VII*	*VII*	*VII*	*VII*	*VIII*
Adjoining vessels	y	y	y	y	y	n	y	y	y
Peripheral	y	y	y	y	y	n	y	y	y
Coronary	y	y	y	y	y	y	y	y	y
Cerebral	y	y	n	n	y	n	n	y	y
Renal	y	y	y	n	y	n	n	y	y
Cardiovascular treatments	n	AH	n	BS	n	n	n	n	n

aortic plaque caps, which had undergone rupture (ulceration), with caps of intact plaques. Caps of ruptured aortic plaques showed a significant increase in macrophage density, an increase in extensibility and a decrease in the ultimate stress when compared with caps from intact plaques. Lee et al. [13,14] performed dynamic and static uniaxial compression tests on aortic plaque caps, which were classified as cellular, hypocellular, and calcified. All caps demonstrated an increase in stiffness with increasing frequencies of stress ranging from 0.05 to 10 Hz. Values of plaque ''moduli'' are presented as a function of the plaque type. McCord [15] performed cyclic bending tests on fresh human arterial ring segments that allowed the passive collapse of an artery, which may occur downstream of a stenosis. The author's studies indicate that cyclic bending and compression may cause artery fatigue and plaque rupture. Lendon et al. [16] show preliminary results of the stress–strain relationships of four (nonulcerated and ulcerated) plaque caps of human aortas. The findings for the caps are very different, the stress–strain curves are qualitatively similar to that of the normal arterial wall. Loree et al. [17] investigated the uniaxial tensile behavior of circumferentially oriented samples of human aortic plaque caps with correlation of the underlying composition (cellular, hypocellular, and calcified). This seems to be the first study where the samples were preconditioned with three cycles at physiological tensile stresses followed by progressive loading until fracture occurred. The authors concluded that the static circumferential tangential modulus of the samples is not significantly affected by the degree of cellularity and calcification determined by histological characterization. Topoleski et al. [18] studied the radial compressive behavior of different plaque compositions of human aorta-iliac arteries segments. Data showed that plaques exhibit composition- and history-dependent nonlinear and inelastic responses under finite deformations. They also found that the area of the hysteresis loop tended to decrease with subsequent cycles. Topoleski and Salunke [19] investigated the multiple cyclic compression and stress-relaxation response of diseased and healthy specimens, while a more recent work [20] demonstrated composition-dependent differences and different responses of plaques to successive relaxation tests in uniaxial compression.

All of these studies have the common limitation that they are based on tests in one direction and that most of the mechanical testing is focused primarily on the properties of the plaque cap, which was isolated from the underlying plaque core and vessel wall. Our aim is to separately quantify the mechanical properties of the different tissue components in the atherosclerotic plaques of human iliac arteries, and to discuss their differences. For this purpose we have performed uniaxial extension tests of human strip samples in two directions (axial and circumferential). Additionally, we report the associated anamnesis, since mechanical properties of arteries depend on several clinical factors. Finally, the ultimate tensile stresses and associated stretches of the different high-grade stenotic arterial segments were investigated. Such systematic direction-dependent and tissue-specific experimental results for human stenotic arteries including ultimate stresses and stretches are not yet available in the literature. These data may serve for theoretically-based quantification in terms of constitutive equations, which can be used in finite element programs to better model the biomechanics of atherosclerotic lesions.

2 Methods

2.1 Material. Iliac arteries are of particular clinical and biomedical interest, since they are atherosclerotic-prone vessels, which frequently undergo endovascular treatments. They are relatively easy to access for vascular diagnostic procedures [21]. Therefore, nine atherosclerotic iliac arteries (I–IX) from eight corpses (74.9 ± 12.5 yrs, mean$\pm$SD) were harvested during autopsy within 24 h from death. From one corpse two arteries (VIII–IX) were obtained. Information about the different types for the iliac arteries and their related anamnesis are summarized in Table 1. The arteries were required to have an atherosclerotic lesion of type *V* or higher according to Stary et al. [22] (for a partitioning of the pathogenesis of atherosclerosis into different stages of plaque formation see Fig. 1 therein). A type *V* lesion (or fibroatheroma), for example, contains mainly reparative smooth muscle cells and fibrous tissue and, additionally, two or more lipid pools of unequal size separated from each other by cells and fibrous tissue. Cross-sectional macroscopic views of the investigated nine stenotic iliac arteries investigated are provided in Figs. 1(a) and 2.

The lesions were classified by a pathologist by means of histological sections and high resolution Magnetic Resonance Images (hrMRI). The specimens were stored in a 4°C calcium-free and glucose-free Tyrode solution (in mmol: NaCl 136.9, KCl 2.7, $MgCl_2$ 1.05, $NaHCO_3$ 11.9, $NaHPO_4$ 0.47, EGTA 2.0). The axial *in situ* prestretch, defined as the ratio of *in situ* length to *ex situ* length, was calculated to be 1.06 ± 0.05. Use of autopsy material from human subjects was approved by the Ethics Committee, Medical University Graz in Austria.

2.2 hrMRI Examination and Histology

2.2.a hrMRI Examination. In order to identify the usability of the harvested arteries in regard to the experimental tests to be performed, and, additionally, to detect the three-dimensional geometry for reconstruction purposes (documented in a follow-up paper), we use **h**igh **r**esolution **m**agnetic **r**esonance imaging. The arteries were tethered with superficial surgical sutures to a grid of nylon threads fixed in a Perspex frame filled with physiological 0.9% NaCl solution maintained at 37°C (see Fig. 1(a) in [23]), and then scanned on a 1.5 T whole body system (Philips ACS-NT,

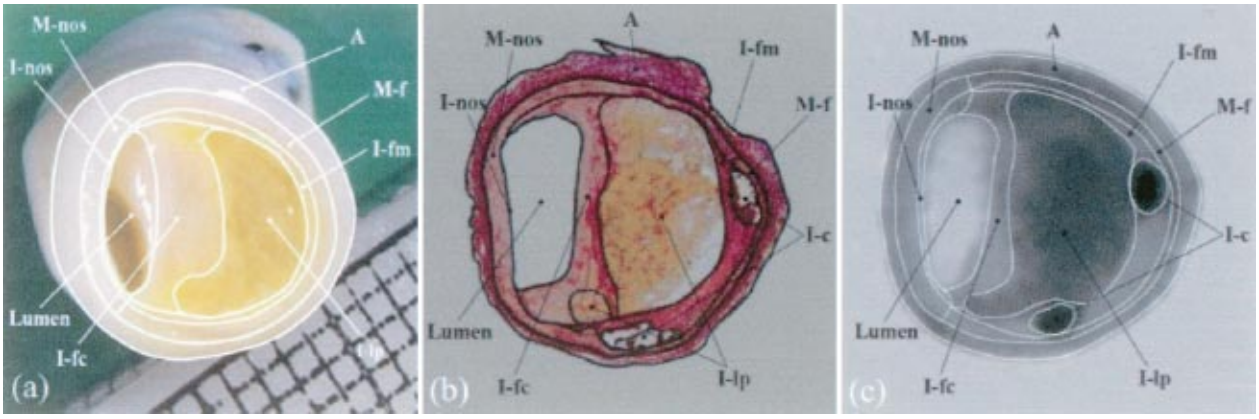

Fig. 1 Human external iliac artery, specimen I: (a) segmented macroscopic view, (b) segmented histological section (EVG coloring)—transmitted light microscopic photograph, (c) high resolution magnetic resonance image of the same artery, filtered and (manually) segmented. The histological section and the magnetic resonance image are taken from the same location.

maximum gradient strength=23 mT) within 24 h after autopsy. The lateral resolution was about 0.25 mm, while the axial resolution was 0.6 mm. Figure 1(c) shows a typical (corrected and noise-filtered) hrMR image of a stenotic artery (specimen I).

After MR-imaging the arteries were marked for histology by injecting black ink at a nylon thread crossing, and then cut through transversely into two halves. One half was used for corresponding histological analyses to allow material characterization, while the other halves of the arteries were dissected anatomically into their major components. We used only lesions that were relatively uniform along their length of about 20 mm. We identified uniformity by means of hrMRI.

2.2.b Histology. The histological analysis is necessary since it allows direct identification the underlying tissue type. The ink-marked half of the vessel segment was fixed in 8% buffered formaldehyde solution (pH 7.4), decalcified with EGTA, embedded in paraffin, and serially sectioned at 0.6 mm intervals. 5 μm thick sections were stained with Elastica van Gieson (EVG) and Hematoxylin and Eosin (H&E). Figure 1(b) shows a transmitted light microscopic photograph of a typical histological section of an external iliac artery (specimen I), which corresponds to the hrMRI cross section shown in Fig. 1(c).

The histological section close by the other half of the artery devoted to anatomical dissection, was segmented by a pathologist, who drew the border of the different tissues on the microphotograph. Eight different tissue types were considered: the nondiseased intima I-nos, (the abbreviation ''nos'' is frequently used in histopathology and stands for **n**ot **o**therwise **s**pecified. In the context of the present study it means ''no appreciable disease,'' or, more precisely ''nonatherosclerotic.''), fibrous cap I-fc (fibrotic part at the luminal border), fibrotic intima at the medial border I-fm, calcification I-c, lipid pool I-lp, nondiseased media M-nos, diseased fibrotic media M-f and adventitia A [6,24]. The histological analysis of the tissue component M-f, i.e. a very thin portion of the media adjacent to the plaque, showed a higher amount of collagenous tissue. Since this tissue component differed in its mechanical behavior from the remaining (nondiseased) portion of the media M-nos, we have considered it in the mechanical test proto-

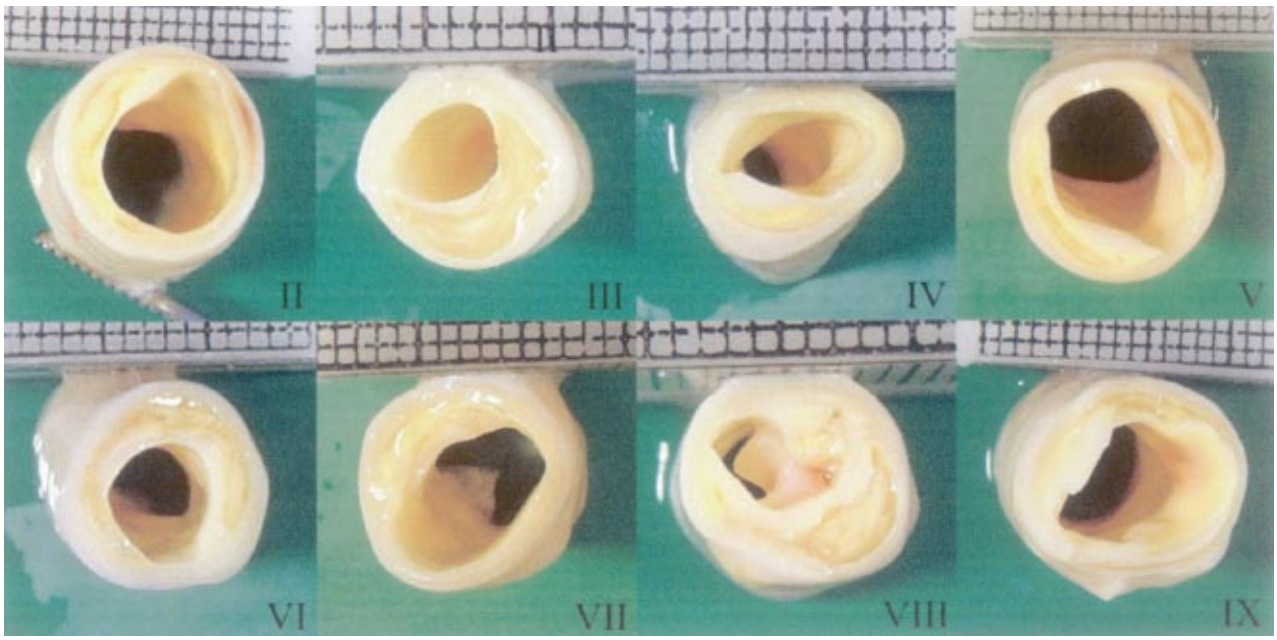

Fig. 2 Macroscopic view of eight human stenotic iliac arteries, specimens II–IX. Top ruler scale: one side of a square characterizes 1 mm.

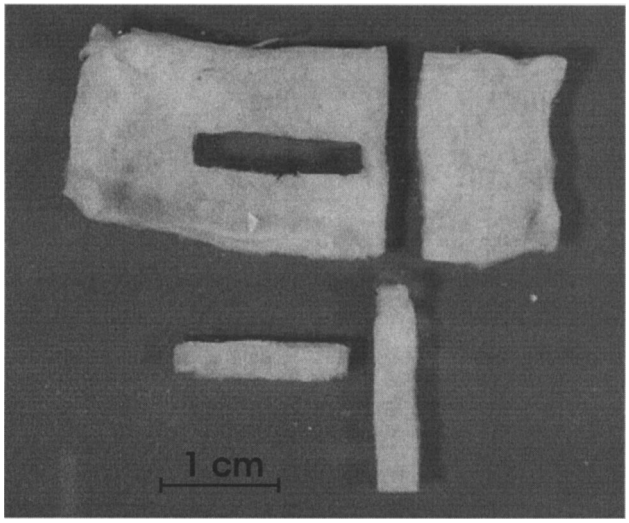

Fig. 3 Representative axial and circumferential strips excised from a dissected adventitial layer.

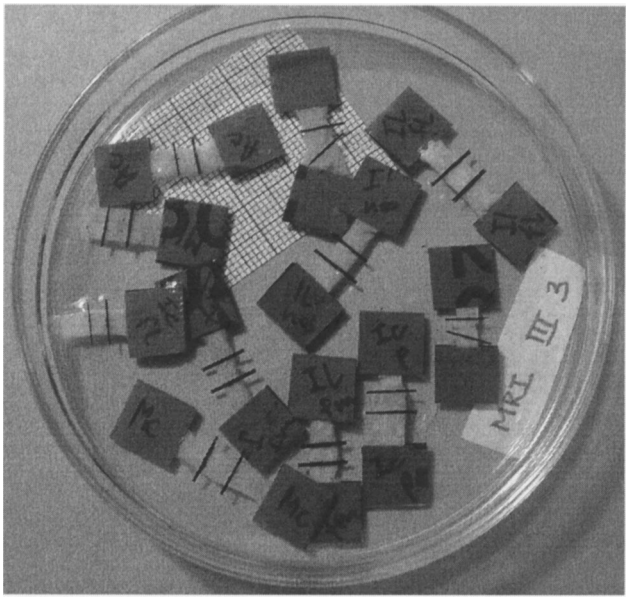

Fig. 4 Eleven strip samples prepared for mechanical testing (from specimen V). Samples of the tissue types A, M-nos, I-nos, I-fc, and I-fm in both directions, and one sample of the calcification I-c in the circumferential direction.

col. Remarkably, for two atherosclerotic lesions we observed morphological features such as calcification with secondary bone formation and typical bone marrow cells. For the mechanism of mineralization during evolution of atherosclerotic plaques see, for example, Ref. [25].

The classification introduced here has served as a basis for the separation of the diseased vessel wall and the segmentation process of the histology (compare with Fig. 1). Each of the tissue components so classified is mechanically relevant and contributes to the overall mechanical response. The separation of the diseased vessel wall was physically feasible using surgical instruments.

2.3 Mechanical Testing. Mechanical tests were performed on a computer-controlled, screw-driven high-precision tensile testing machine. The system was based on a commercial class 1 machine (Messphysik, μ-Strain Instrument ME 30-1, Fürstenfeld, Austria), which was adapted for small biological specimens by integrating a tissue bath at (37 ± 0.1)°C maintained by a heater-circulation unit (model E 200, Lauda; Lauda-Königshofen, Germany). The crossheads are driven in opposing directions, allowing a fixed position of the sample center. A crosshead stroke resolution of 0.04 μm and a minimum load resolution of 1 mN using a 25 N load cell is specified by the manufacturer. Gauge length and width are measured optically using a PC-based CCD-camera videoextensometer that allows automatic gauge mark and edge recognition. Dimensional measurements are performed with a total resolution of 16 bit with regard to the camera's field of view.

The lipid pools I-lp and the bone marrows were excluded from mechanical testing. The lipid pool was not tested because of its liquid (''butter-like'') consistence, while the bone marrow was not tested because of its small size. The lipid pools are assumed to behave as a nearly incompressible fluid [24,26–28] not able to sustain shear stress [29].

For the determination of the passive, quasistatic stress–stretch response of the individual tissue components, rectangular strip samples with axial and circumferential orientations were excised from the specimen. Representative axial and circumferential strips from a dissected adventitial layer are shown in Fig. 3. The samples varied from 7 to 17 mm in length, from 2.2 to 5.6 mm in width, and from 0.24 to 1.7 mm in thickness. Pieces of emery paper were attached to the ends of the samples to prevent slippage during testing. Two black colored straw chips were glued transversely in parallel onto the middle part of the samples to act as gauge markers for the axial deformation measurements. The strip samples were allowed to equilibrate for 30–60 min in a calcium-free physiological 0.9% NaCl solution at 37°C. A collection of strip samples from specimen V, which were prepared for mechanical testing, is illustrated in Fig. 4.

Preconditioning was achieved by executing up to five successive loading–unloading cycles for each test. Then the samples underwent one cyclic quasistatic uniaxial extension test with continuous recording of tensile force, width and gauge length at a constant crosshead speed of 1 mm/min. Finally, the strain was increased until fracture occurred. Sometimes it happened that the fracture occurred outside the gauge section of the sample close to one of the grips so that another sample was prepared and tested if enough material was available. It was usually possible to get a second sample for the tissue types A, M-nos and I-fc. A photograph of a fractured tissue component is shown in Fig. 5. A total number of 107 samples were tested, and 82 are documented in the present paper (18 for A, 18 for M-nos, 12 for I-nos, 17 for I-fc, 8 for I-fm, 5 for M-f, and 4 for I-c). The four I-c samples were

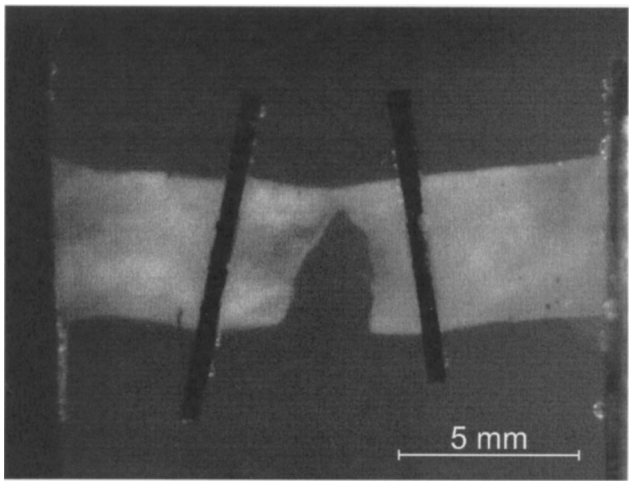

Fig. 5 Representative photograph of a fractured tissue component (specimen I), nondiseased intima I-nos tested in the circumferential direction.

obtained from three specimens, i.e. I (samples in both directions), IV (sample in axial direction), and V (sample in circumferential direction). After tensile testing the sample's thickness was measured by means of the videoextensometer.

The stretch ratio λ was computed as l/L, where l and L are the measured gauge lengths in the loaded and unloaded configurations, respectively. Based on the global equilibrium, the incompressibility condition, and the experimental data, it is straightforward to compute the associated Cauchy stress, denoted as σ. Incompressibility requires $LWT=lwt$, where w, t and W, T are the width and the thickness of the strip sample in the loaded and unloaded configurations, respectively. Thus, $\sigma=f/wt$, and, therefore,

$$\sigma=\frac{f}{WT}\lambda, \tag{1}$$

where f is the actual tensile force. Hence, the computation of σ requires the measurements of the five parameters f, W, T, l, L. The Cauchy stresses were then plotted versus the stretch ratio.

Finally, we compute the hysteresis loop area $A\in[0,100]$ within a typical loading–unloading cycle defined to be $A=100(A_l-A_u)/A_l$, where A_l is the area below the σ/λ-curve during tissue loading, and A_u is the area below the σ/λ-curve during unloading.

3 Results

Table 1 documents the anamnesis of the donors from which the specimens I–IX were obtained. The set of specimens consists of five common iliac arteries (CIA), three internal iliac arteries (IIA), and one external iliac artery (EIA). The table documents data on age, sex, primary disease, cause of death, type of atherosclerotic lesions, and cardiovascular treatments. Moreover, the condition of the adjoining vessels and the remaining parts of the arterial vasculature in regard to atherosclerosis is shown. These factors were proven to affect the mechanical properties of arteries (see, for example, the review [30]), and are important for a complete registration of arterial mechanics of aged patients.

Figure 1 illustrates the marked heterogeneity of a lesion and the good correlation between the different images. In a comparative study Figs. 6 and 7 exhibit the highly nonlinear and anisotropic (except for the fibrotic intima at the medial border I-fm) mechanical responses, i.e. Cauchy stress versus stretch, of the different tissue types (A, M-nos, M-f, I-nos, I-fc, and I-fm) of the investigated specimens I–IX. In particular, a comparison is provided between the responses in the circumferential direction and in the axial direction. The loading–unloading paths showed only small hysteresis (Table 2), and, therefore, the unloading path is not shown in the plots. Some measurements of the samples close to the fracture appeared to be rather noisy and are not shown in the plots. Only for the adventitia A and the nondiseased media M-nos were complete sets of strip samples from all specimens available (Figs. 6(a)–6(d)). For the diseased fibrotic media M-f, unfortunately, only five sample could be tested (Figs. 6(c), 6(d)). The calcification I-c has shown very stiff and linear mechanical responses (not shown in the plots) with an average Young's modulus of 12.6 ± 4.7 MPa, mean$\pm$SD.

The ultimate tensile stress characterizes the maximum resistance to fracture. It is equivalent to the maximum load that can be carried by the cross-sectional area when the load is applied as a tensile force, see Eq. (1). The ultimate tensile stresses (in kPa) and the associated ultimate stretches, denoted as σ_{ult} and λ_{ult}, of all tested samples that fractured within the gauge section are summarized in Table 3. Values that are related to samples tested in the circumferential direction are denoted by c, and to samples tested in axial direction by a. Missing values indicate either that the test was unsatisfactory or that a sample was not available. The ultimate values in the table are related to the plots of the samples shown in Figs. 6 and 7. Furthermore, the mean values and the standard deviations (SD) of the ultimate tensile stresses, denoted as $\overline{\sigma}_{\text{ult}}$, and the ultimate stretches, denoted as $\overline{\lambda}_{\text{ult}}$, are documented. The calcification has shown an average ultimate tensile stress of 179 ± 56 kPa, mean$\pm$SD at an average stretch of 1.02 ± 0.005, mean$\pm$SD.

4 Discussion

Histopathological investigations suggested that plaque rupture involves plaque cap failure. Therefore, most of the mechanical studies focused primarily on the properties of fibrous plaque caps. However, plaque stability cannot be dependent only on the mechanical properties of the plaque cap. The stress distribution in the plaque cap is strongly influenced by all surrounding components of the atherosclerotic lesion so that a systematic, direction-dependent and tissue-specific experimental testing is needed. Even the adventitia is in strong interaction with the plaque cap and plays a crucial role in plaque loading. Recent studies have shown that for aged human arteries the adventitia is a significant carrying structure [31], and that disrupted plaques exhibit increased incidence of adventitia inflammation [32]. This is the reason why we investigated the mechanical properties of different tissue components in human atherosclerotic plaques and the healthy surrounding tissues. Lendon et al. [12] showed that the mechanical properties of human aortic intima did not significantly alter when stored at 4°C for time periods up to 64 h. Berberian and Fowler [33] showed that minimal enzymatic changes occur in rabbit aortas within 48 h when stored at 4°C. For this reason all mechanical tests were finished within 48 h after autopsy.

Knowledge of the mechanical properties of atherosclerotic plaque is of fundamental importance for identifying plaque rupture, the most common antecedent of myocardial infarction. In this study we have investigated the mechanical properties of nine atherosclerotic lesions—their mechanical responses indicate significant variations, as seen in the plots of Figs. 6 and 7. All tissue components investigated, with the exception of the calcification I-c, show a highly nonlinear behavior, which was also found for aortic fibrous caps in the studies by, for example, Lendon et al. [16] and Loree et al. [17]. Because of the nonlinear responses of the tissues a measure of stiffness would only be meaningful for certain stress or stretch levels, not provided here. Several authors found, however, that diseased arterial tissue is stiffer than healthy tissue (see Born and Richardson [11], Topoleski et al. [18] among others). In regard to our study, by comparing the slopes of the stress–stretch curves at low and high stresses there is a clear tendency that diseased tissues are stiffer than healthy ones. For example, all diseased fibrotic media M-f tested are stiffer than the nondiseased samples M-nos (see Figs. 6(c), 6(d)); there is also a clear tendency that the diseased intima tissue (fibrous cap I-fc and I-fm) is stiffer than the nondiseased tissue I-nos (compare with Figs. 6(e), 6(f), and Fig. 7).

The present plots allow also a unique and interesting comparison of the mechanical response of a sample oriented and tested in the circumferential direction with the associated sample oriented and tested in the axial direction. For example, as can be seen from Figs. 6(c), 6(d), the mechanical response of the healthy media M-nos in the axial direction tends to be weaker than in the circumferential direction, in which the smooth muscle cells are mainly oriented [34] (samples from specimens III, VII, and IX exhibit a stiffer response in the axial direction). The fibrotic media M-f tested show also a weaker behavior in the axial direction than in the circumferential direction (labeled as I-f, VIII-f in the plots of Figs. 6(c), 6(d)), where, however, only two comparable samples were available for testing. The adventitia A (Figs. 6(a), 6(b)), the nondiseased intima I-nos (Figs. 6(e), 6(f)) and the fibrous caps I-fc (Figs. 7(a), 7(b)) tested in the axial direction indicate the tendency to be stiffer than associated samples in the circumferential direction. Interestingly, as can be seen from Figs. 6(a), 6(b), all samples of the adventitia tested demonstrate a similar, very high stiffness behavior in the high-stress domain.

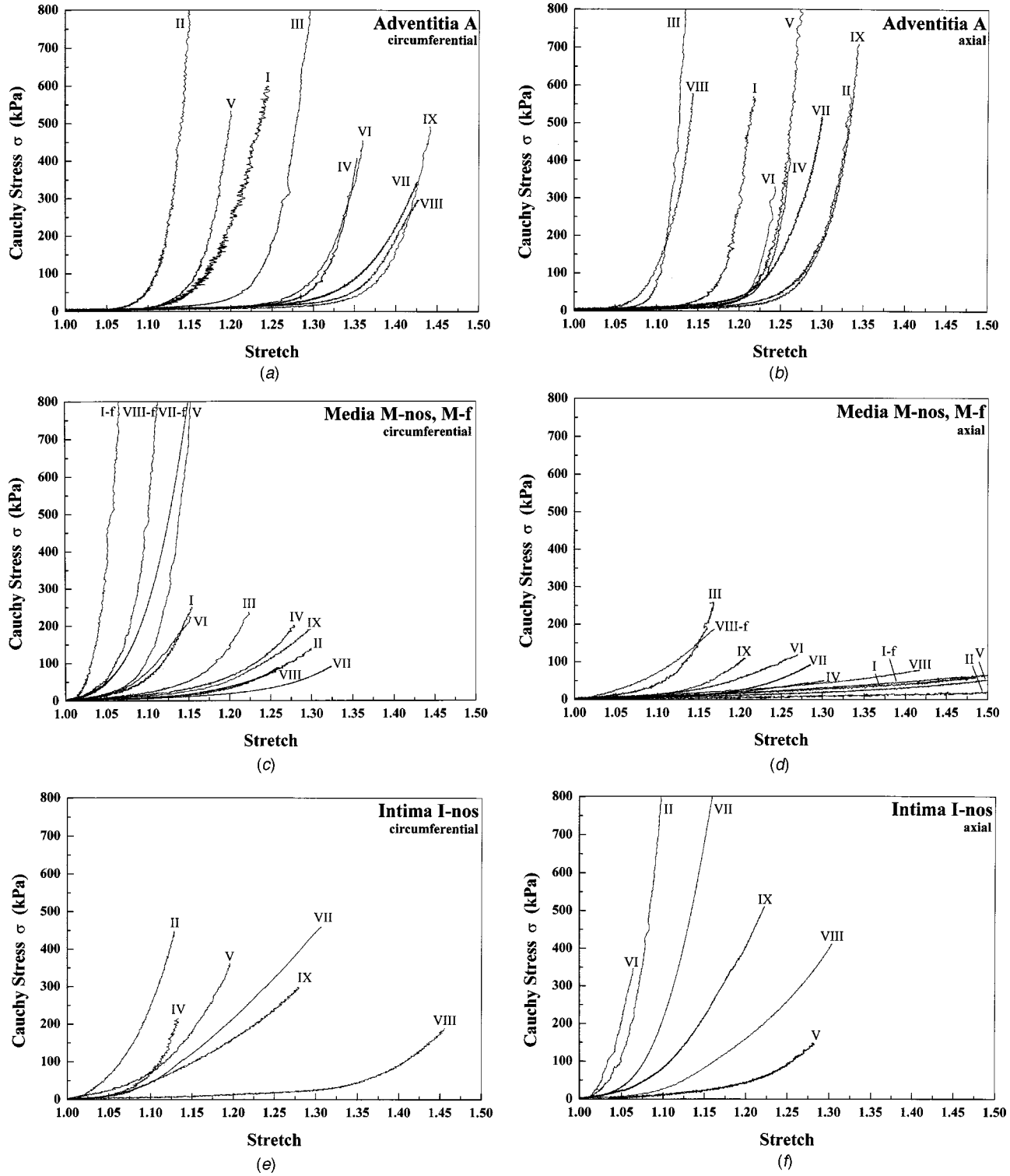

Fig. 6 Uniaxial tensile stress–stretch responses of different human tissues in the circumferential and axial directions. (a), (b) are stress–stretch plots for the adventitia A, (c), (d) are plots for the healthy and diseased media (M-nos and M-f), and (e), (f) are related to the healthy intima I-nos. Labels I-f, VII-f, and VIII-f in (c), (d), indicate fibrotic media samples from specimens I, VII, and VIII, respectively.

Strip samples of the fibrotic intima at the medial border I-fm show almost isotropic behavior for all comparable samples obtained from specimens III, V, and VI (Figs. 7(c), 7(d)). The sample from specimen VI obtained from a 60 year old male donor (IIA) shows almost the same behavior as the sample from specimen V obtained from a 81 year old female donor (CIA).

Our study indicates that the calcification I-c has about the same stiffness as that of the stiffest tissue component tested, i.e., the adventitia A in both directions or the diseased fibrotic media M-f in the circumferential direction in the high stress domain at which the response is almost linear. All other tissues show a softer mechanical response than the calcification does. By defining a plaque

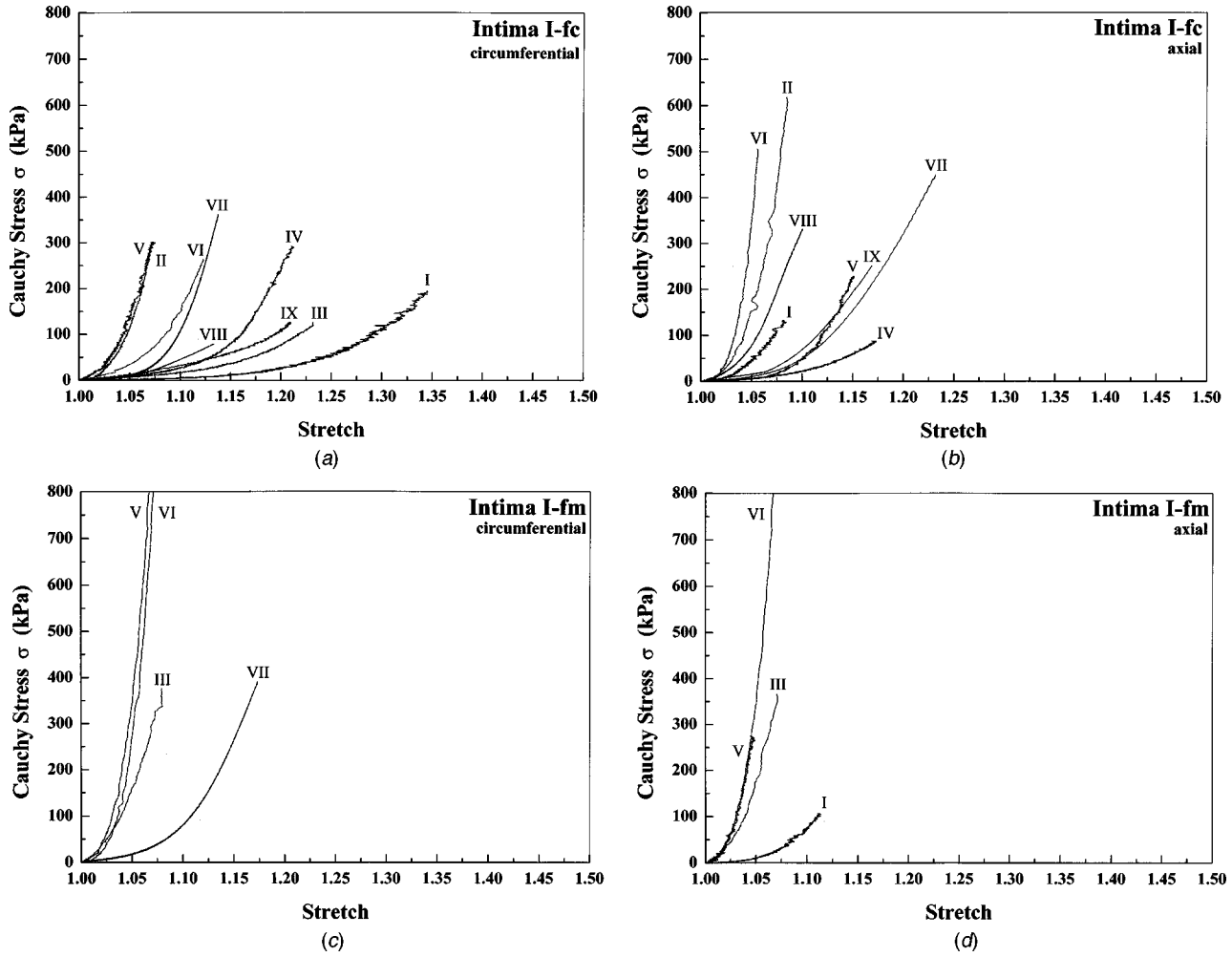

Fig. 7 Uniaxial tensile stress–stretch responses of different human tissues in the circumferential and axial directions. (a), (b) are stress–stretch plots for the fibrous cap I-fc, while (c), (d) are plots for the fibrotic intima samples at the medial border I-fm.

''moduli'', Lee et al. [13] found that calcified caps of abdominal aortic plaques are 4–5 times stiffer than cellular caps in radial compression tests at room temperature.

In our study, the adventitia A shows the highest average ultimate tensile stresses $\overline{\sigma}_{\text{ult}}$, while the nondiseased media M-nos shows the lowest average values (for this comparison the diseased fibrotic media M-f was excluded since ultimate values of only four samples were available); see Table 3. It is the adventitia, which demonstrates very high average tensile strength having significant load-carrying capabilities at higher pressures at which it changes to a stiff ''jacket-like'' tube, that prevents the smooth muscle from acute overdistension (see also [9,31]). From the mechanical perspective, it is the nondiseased media that is the most significant (load-carrying) layer in a healthy artery under physiological conditions.

The average ultimate tensile stress $\overline{\sigma}_{\text{ult}}$ of fibrous caps I-fc in the circumferential direction was 254.8 ± 79.8 kPa at an associated stretch of 1.182 ± 0.1. The stress values are in good agreement with stress values obtained by, for example, Lendon et al. [12], who have performed uniaxial tensile tests on strips from human ulcerated aortic plaques in the circumferential direction. However, the associated stretch values they obtained were about 1.5, which deviate significantly from our findings. Cheng et al. [35] reported maximum circumferential stresses of 545 ± 160 kPa in human fibrous caps that ruptured. These (indistinct) values were calculated by means of a linear elastic finite element analyses without a failure criterion. Thereby, ruptured lesions were discretized and a mean intraluminal pressure of 110 mmHg applied. The ultimate tensile stresses of human aortic fibrous caps in the circumferential direction investigated by Loree et al. [17] ranged from 149 to 701

Table 2 Calculated mean values in (%) and associated standard deviation (SD) of the hysteresis loop area of all tissue types (obtained from specimens I–IX) tested in the circumferential direction *c* and the axial direction *a*

	Tissue type											
	A		M-nos		M-f		I-nos		I-fc		I-fm	
Hysteresis (%)	*c*	*a*	*c*	*a*	*c*	*a*	*c*	*a*	*c*	*a*	*c*	*a*
Mean	17.3	13.6	13.8	8.8	5.8	4.7	12.8	7.9	16.7	13.1	11.1	10.6
SD	9.1	6.3	9.8	3.1	5.4	3.0	7.1	5.4	3.9	5.2	6.1	8.6

Table 3 Ultimate tensile stress σ_{ult} (kPa) and associated ultimate stretch λ_{ult} (1) of the different types of tissue of all specimens I–IX tested in the circumferential direction *c* and the axial direction *a*. Associated mean values $\bar{\sigma}_{ult}$ and $\bar{\lambda}_{ult}$ and standard deviations (SD).

		Tissue type											
		A		M-nos		I-nos		I-fc		I-fm		M-f	
Specimen		*c*	*a*	*c*	*a*	*c*	*a*	*c*	*a*	*c*	*a*	*c*	*a*
I	σ_{ult}	618.5	737.6	261.5	183.7			205.6	509.8		171.8	1278.1	181.5
	λ_{ult}	1.243	1.223	1.156	1.863			1.374	1.121		1.135	1.076	1.797
II	σ_{ult}	832.3	667.6	212.9	128.4	435.2	1321.9	299.3	617.5				
	λ_{ult}	1.173	1.392	1.409	2.005	1.129	1.117	1.073	1.068				
III	σ_{ult}	1188.3	1276.6	229.7	261.6			126.4			366.5		
	λ_{ult}	1.479	1.157	1.249	1.169			1.232			1.071		
IV	σ_{ult}	845.4	886.6	201.6				292.2					
	λ_{ult}	1.424	1.299	1.280				1.213					
V	σ_{ult}		990.7		432.7	356.4		301.3		941.1	294.3		
	λ_{ult}		1.282		1.830	1.201		1.076		1.071	1.057		
VI	σ_{ult}	802.3		298.2	121.8			287.9	506.1	999.2			
	λ_{ult}	1.413		1.177	1.283			1.126	1.058	1.078			
VII	σ_{ult}	1479.5		108.9	92.5	473.9	796.2	360.1	449.2	390.1		869.0	
	λ_{ult}	1.676		1.323	1.284	1.320	1.159	1.138	1.232	1.173		1.154	
VIII	σ_{ult}	1090.1	1005.3	93.7	141.3	368.2	703.8		402.3				193.2
	λ_{ult}	1.458	1.458	1.260	1.583	1.648	1.435		1.121				1.176
IX	σ_{ult}	1396	1097.9	209.9	148.1	809.1	952.9	165.8	326.9				
	λ_{ult}	1.652	1.658	1.313	1.267	1.357	1.309	1.222	1.208				
mean	$\bar{\sigma}_{ult}$	1031.6	951.8	202.0	188.8	488.6	943.7	254.8	468.6	776.8	277.5	1073.6	187.4
SD		306.8	209.0	69.8	110.9	185.6	272.3	79.8	100.1	336.2	98.4	289.3	8.3
mean	$\bar{\lambda}_{ult}$	1.440	1.353	1.270	1.536	1.331	1.255	1.182	1.135	1.107	1.088	1.115	1.487
SD		0.175	0.168	0.081	0.327	0.199	0.146	0.100	0.071	0.057	0.042	0.055	0.439

kPa, with a mean of 484 ± 216 kPa and the ultimate tensile stretches ranged from 1.15 to 1.60, with a mean ultimate tensile stretch of 1.30 ± 0.16. Limitations in this study were the small number of specimens (six) that fractured within the gauge section and that uniaxial testing was performed at room temperature.

It turns out that of all intimal tissues investigated (I-nos, I-fc, and I-fm) the lowest fracture stress is for the fibrous cap in the circumferential direction, which supports the hypothesis of Richardson et al. [29] that peak circumferential stress may be a critical factor in plaque rupture. Interestingly, both the stress and stretch at calcification I-c fracture, i.e., 179 ± 56 kPa and 1.02 ± 0.005, respectively, are smaller than for each of the other tissues tested. Except for the medial tissues M-nos and M-f, all others show, on average, higher ultimate tensile stretches $\bar{\lambda}_{ult}$ in the circumferential direction than in the axial direction.

Table 2 shows the mean areas of the hysteresis loops for all tissue types tested. Remarkably, all tissue components oriented in the circumferential direction show a larger hysteresis than those oriented in the axial direction.

Limitations of our study concern the number of samples tested, which were too small in order to recognize age-specific, gender-specific, artery type-specific or atherosclerotic type-specific differences of the mechanical properties. In addition, due to the small size of the specimen, appropriate strip samples could not always be prepared. It was especially difficult to get samples from the fibrotic media M-f, because the M-f is a very thin tissue located behind the fibrous intima at the medial border I-fm. A possible improvement in measurement of the tensile properties of micro-sized specimens would be the use of micro-testers. Quite a number of fracture tests failed in the sense that the fracture occurred outside the gauge section, although a second sample could sometimes be prepared and tested. Due to the small size of many strip samples the idea of running experiments with dumbbell shaped samples would also not have been successful.

5 Conclusion

This study has attempted to systematically investigate and quantify the anisotropic mechanical responses of the different tissue components of nine human stenotic iliac arteries selected by means of MRI; associated anamnesis of donors were reported. From anatomical dissections into eight different tissue types, which were based on histological images, a total number of 107 samples could be obtained for experimental tensile testing at a temperature of 37°C. Gauge length and width were appropriately measured optically using a PC-based CCD-camera videoextensometer. Novel direction-dependent stress–strain data and fracture stress and stretch of all plaque types and healthy surrounding tissues are described.

This approach presents a step toward a better understanding of the biomechanical behavior of atherosclerotic lesions as a function of their components; however, because of the variability of the lesions and their marked heterogeneity the need for more data remains. The data presented indicate the general characteristics of the mechanical response of individual arterial tissue types and may serve as a basis for the design of related constitutive models, a task that is performed in an upcoming paper. The present study shows the need for anisotropic models and may help to perform computational analyses of plaques within mechanical interventional therapies such as balloon angioplasty with greater accuracy.

Acknowledgments

The authors are indebted to Professor R. Stollberger from the division for clinical and experimental magnetic resonance research at the Medical University Graz for his cooperation in developing appropriate MR sequences for high resolution plaque imaging. Thanks also go to C.A.J. Schulze-Bauer and E. Pernkopf for contributions to the experimental tests. Financial support for this research was provided by the Fonds zur Fortsetzung Christian's Forschung and by the Austrian Science Foundation under START-Award Y74-TEC. This support is gratefully acknowledged.

Nomenclature

A = adventitia
CIA = common iliac artery
EIA = external iliac artery
f = tensile force

hrMRI = high resolution Magnetic Resonance Imaging
IIA = internal iliac artery
I-c = calcification
I-fc = fibrous cap
I-fm = fibrotic intima at the medial border
I-lp = lipid pool
I-nos = nondiseased intima
L, l = gauge length in the load-free (reference) and current configurations
M-f = diseased fibrotic media
M-nos = nondiseased media
SD = standard deviation
T, t = thickness in the load-free (reference) and current configurations
W, w = width of the strip sample in the load-free (reference) and current configurations
λ = stretch ratio
σ = Cauchy stress
σ_{ult}, λ_{ult} = ultimate tensile stress and associated ultimate stretch
$\overline{\sigma}_{ult}$, $\overline{\lambda}_{ult}$ = mean values of the ultimate tensile stresses and associated ultimate stretches

References

[1] Fuster, V., editor, 2002, *Assessing and Modifying the Vulnerable Atherosclerotic Plaque: American Heart Association*, Futura Publishing Company, Armonk.

[2] Kramer, C. M., 2002, ''Magnetic Resonance Imaging to Identify the High-Risk Plaque,'' Am. J. Cardiol., **90**, pp. 15L–17L.

[3] Virmani, R., Burke, A. P., Kolodgie, F. D., and Farb, A., 2003, ''Pathology of the Thin-Cap Fibroatheroma: A Type of Vulnerable Plaque,'' J. Invas. Cardiol., **16**, pp. 267–272.

[4] Kavey, R. W., Daniels, S. R., Lauer, R. M., Atkins, D. L., Hayman, L. L., and Taubert, K., 2003, ''American Heart Association Guidelines for Primary Prevention of Atherosclerotic Cardiovascular Disease Beginning in Childhood,'' Circulation, **107**, pp. 1562–1566.

[5] Rayner, M., and Petersen, S., 2000, *European Cardiovascular Disease Statistics 2000*, British Heart Foundation (BHF), London.

[6] Holzapfel, G. A., Stadler, M., and Schulze-Bauer, C. A. J., 2002, ''A Layer-Specific Three-Dimensional Model for the Simulation of Balloon Angioplasty Using Magnetic Resonance Imaging and Mechanical Testing,'' Ann. Biomed. Eng., **30**, pp. 753–767.

[7] Richardson, P. D., 2002, ''Biomechanics of Plaque Rupture: Progress, Problems, and New Frontiers,'' Ann. Biomed. Eng., **30**, pp. 524–536.

[8] Salunke, N. V., and Topoleski, L. D. T., 1997, ''Biomechanics of Atherosclerotic Plaque,'' Crit. Rev. Biomed. Eng., **25**, pp. 243–285.

[9] Humphrey, J. D., 2002, *Cardiovascular Solid Mechanics: Cells, Tissues, and Organs*, Springer-Verlag, New York.

[10] Lendon, C. L., Briggs, A. D., Born, G. V. R., Burleigh, M. C., and Davies, M. J., 1988, ''Mechanical Testing of Connective Tissue in the Search for Determinants of Atherosclerotic Plaque Cap Rupture,'' Biochem. Soc. Trans., **16**, pp. 1032–1033.

[11] Born, G. V. R., and Richardson, P. D., 1990, ''Mechanical Properties of Human Atherosclerotic Lesions,'' *Pathology of Human Atherosclerotic Plaques*, edited by S. Glagov, W. P. Newman, and S. A. Schaffer, Springer-Verlag, New York, pp. 413–423.

[12] Lendon, C. L., Davies, M. J., Born, G. V. R., and Richardson, P. D., 1991, ''Atherosclerotic Plaque Caps are Locally Weakened When Macrophages Density is Increased,'' Atherosclerosis, **87**, pp. 87–90.

[13] Lee, R. T., Grodzinsky, A. J., Frank, E. H., Kamm, R. D., and Schoen, F. J., 1991, ''Structure-Dependent Dynamic Mechanical Behavior of Fibrous Caps From Human Atherosclerotic Plaques,'' Circulation, **83**, pp. 1764–1770.

[14] Lee, R. T., Richardson, S. G., Loree, H. M., Grodzinsky, A. J., Gharib, S. A., Schoen, F. J., and Pandian, N., 1992, ''Prediction of Mechanical Properties of Human Atherosclerotic Tissue by High-Frequency Intravascular Ultrasound Imaging,'' Arterioscler. Thromb., **12**, pp. 1–5.

[15] McCord, B. N., 1992, ''Fatigue of Atherosclerotic Plaque,'' Ph.D. thesis, Department of Mechanical Engineering, Georgia Institute of Technology, GA.

[16] Lendon, G. L., Davies, M. J., Richardson, P. D., and Born, G. V. R., 1993, ''Testing of Small Connective Tissue Specimens for the Determination of the Mechanical Behavior of Atherosclerotic Plaques,'' J. Biomed. Eng., **15**, pp. 27–33.

[17] Loree, H. M., Grodzinsky, A. J., Park, S. Y., Gibson, L. J., and Lee, R. T., 1994, ''Static Circumferential Tangential Modulus of Human Atherosclerotic Tissue,'' J. Biomech., **27**, pp. 195–204.

[18] Topoleski, L. D. T., Salunke, N. V., Humphrey, J. D., and Mergner, W. J., 1997, ''Composition- and History-Dependent Radial Compressive Behavior of Human Atherosclerotic Plaque,'' J. Biomed. Mater. Res., **35**, pp. 117–127.

[19] Topoleski, L. D. T., and Salunke, N. V., 2000, ''Mechanical Behavior of Calcified Plaques: A Summary of Compression and Stress-Relaxation Experiments,'' Z. Kardiol Suppl., **89**, Suppl. 2, pp. II/85–II/91.

[20] Salunke, N. V., Topoleski, L. D. T., Humphrey, J. D., and Mergener, W. J., 2001, ''Compressive Stress-Relaxation of Human Atherosclerotic Plaque,'' J. Biomed. Mater. Res., **55**, pp. 236–241.

[21] Schulze-Bauer, C. A. J., Mörth, C., and Holzapfel, G. A., 2003, ''Passive Biaxial Mechanical Response of Aged Human Iliac Arteries,'' J. Biomech. Eng., **125**, pp. 395–406.

[22] Stary, H. C., 2003, *Atlas of Atherosclerosis: Progression and Regression*, The Parthenon Publishing Group Limited, Boca Raton, London, New York, Washington, D.C., 2nd ed.

[23] Schulze-Bauer, C. A. J., and Holzapfel, G. A., 2003, ''Determination of Constitutive Equations for Human Arteries From Clinical Data,'' J. Biomech., **36**, pp. 185–169.

[24] Holzapfel, G. A., Schulze-Bauer, C. A. J., and Stadler, M., 2000, ''Mechanics of Angioplasty: Wall, Balloon, and Stent,'' *Mechanics in Biology*, edited by J. Casey and G. Bao, The American Society of Mechanical Engineers (ASME), New York, AMD-Vol. 242/BED-Vol. 46, pp. 141–156.

[25] Demer, L. L., 1995, ''A Skeleton in the Atherosclerosis Closet,'' Circulation, **92**, pp. 2029–2032.

[26] Loree, H. M., Kamm, R. D., Stringfellow, R. G., and Lee, R. T., 1992, ''Effects of Fibrous Cap Thickness on Peak Circumferential Stress in Model Atherosclerotic Vessels,'' Circ. Res., **71**, pp. 850–858.

[27] Loree, H. M., Tobias, B. J., Gibson, L. J., Kamm, R. D., Small, D. M., and Lee, R. T., 1994, ''Mechanical Properties of Model Atherosclerotic Lesion Lipid Pools,'' Arterioscler. Thromb., **14**, pp. 230–234.

[28] Williamson, S. D., Lam, Y., Younis, H. F., Huang, H., Patel, S., Kaazempur-Mofrad, M. R., and Kamm, R. D., 2003, ''On the Sensitivity of Wall Stresses in Diseased Arteries to Variable Material Properties,'' J. Biomech. Eng., **125**, pp. 147–155.

[29] Richardson, P. D., Davies, M. J., and Born, G. V. R., 1989, ''Influence of Plaque Configuration and Stress Distribution on Fissuring of Coronary Atherosclerotic Plaques,'' Lancet, **2(8669)**, pp. 941–944.

[30] Hickler, R. B., 1990, ''Aortic and Large Artery Stiffness: Current Methodology and Clinical Correlations,'' Clin. Cardiol., **13**, pp. 317–322.

[31] Schulze-Bauer, C. A. J., Regitnig, P., and Holzapfel, G., 2002, ''Mechanics of the Human Femoral Adventitia Including High-Pressure Response,'' Am. J. Physiol., **282**, pp. H2427–H2440.

[32] Moreno, P. R., Purushothaman, K. R., Fuster, V., and O'Connor, W. N., 2002, ''Intimomedial Interface Damage and Adventitial Inflammation is Increased Beneath Disrupted Atherosclerosis in the Aorta: Implications for Plaque Vulnerability,'' Circulation, **105**, pp. 2504–2511.

[33] Berberian, P. A., and Fowler, S., 1979, ''The Subcellular Biochemistry of Human Arterial Lesions. I. Biochemical Constituents and Marker Enzymes in Diseased and Unaffected Portions of Human Aortic Specimens,'' Exp. Mol. Pathol., **30**, pp. 27–40.

[34] Rhodin, J. A. G., 1980, ''Architecture of the Vessel Wall,'' *Handbook of Physiology, The Cardiovascular System*, edited by D. F. Bohr, A. D. Somlyo, and H. V. Sparks, 2, American Physiologial Society, Bethesda, Maryland, pp. 1–31.

[35] Cheng, G. C., Loree, H. M., Kamm, R. D., Fishbein, M. C., and Lee, R. T., 1993, ''Distribution of Circumferential Stress in Ruptured and Stable Atherosclerotic Lesions: A Structural Analysis With Histopathological Correlation,'' Circulation, **87**, pp. 1179–1187.